Svedberg Open
DISSEMINATION OF KNOWLEDGE

International Journal of Artificial Intelligence and Machine Learning

Publisher's Home Page: https://www.svedbergopen.com/

Research Paper Open Access

Cross-Sector Risk Forecasting Using Federated Machine Learning: Applications in Finance, Healthcare and Urban Planning

Md Arif Hossain[1*], S M Arif Al Sany[2], Ridwanur Rahman[2], Molla Al Rakib Hasan[2]

[1]College of Business, University of the Cumberlands, Williamsburg, Kentucky, United States
[2]College of Business, Lamar University, Beaumont, Texas, United States
Corresponding Author: Md Arif Hossain (mhossain50907@ucumberlands.edu)

Abstract
Federated learning has emerged as a potential paradigm for collaborative intelligence because it allows many businesses to train machine learning models together without sharing raw data. However, traditional federated learning algorithms frequently assume homogenous data distributions and shared feature spaces, which limits their application to diverse cross-domain contexts. This study introduces a Personalized Federated Proximal (FedProx) architecture for collaborative risk forecasting in three distinct sectors: finance, healthcare, and urban planning. The suggested architecture includes sector-specific input adapters, a shared residual backbone, private residual adapters, and task-specific prediction heads to strike a compromise between collaborative knowledge sharing and domain-specific expertise. Adaptive sector-weighted aggregation is used to improve global model optimization while maintaining local characteristics. The framework is tested on publicly available datasets using a rigorous process that includes five random seeds and three rolling temporal folds for urban forecasting, totaling 15 repeated trials. Performance is measured using Accuracy, Balanced Accuracy, F1-score, Matthews Correlation Coefficient (MCC), ROC-AUC, and PR-AUC. Experimental results reveal that the proposed framework performs similarly to the Sector FedAvg baseline in financial risk forecasting while consistently improving urban forecasting, particularly in ROC-AUC and PR-AUC. Although healthcare remains a difficult prediction problem due to the complexity of the leakage-safe composite target, the suggested strategy improves overall classification accuracy while retaining consistent performance across multiple experiments. These findings show that personalized federated learning is a viable method for collaborative risk prediction across diverse application domains while limiting negative transfer via sector-specific adaptation.

Keywords: Federated Learning, Personalized FedProx, Cross-Sector Learning, Risk Forecasting, Financial Risk Prediction, Healthcare Analytics, Urban Planning, Privacy-Preserving Machine Learning.

1. Introduction

The increasing pace of digital transformation of contemporary society has resulted in the widespread use of intelligent information systems in a variety of application fields, including financial services, healthcare, and urban infrastructure. Banking transactions, electronic health records, wearable devices, environmental sensors, and Internet of Things (IoT) platforms all generate massive amounts of heterogeneous data on a continual basis. The capacity to successfully evaluate such distributed data has made risk forecasting a critical component of decision support, allowing firms to anticipate unfavourable events, optimize resource allocation, and improve operational resilience. Accurate prediction of financial defaults, high-risk patients, and environmental risks decreases economic losses while simultaneously improving public safety and service quality. As a result, data-driven risk forecasting has emerged as a key study topic in artificial intelligence, machine learning, and data analytics [1, 2].

Despite having the same goal of anticipating future dangers, financial, healthcare, and urban planning systems have significantly distinct data properties. Financial datasets often contain structured numerical and categorical data about client demographics, credit history, loan characteristics, and repayment behaviour, with the main goal of estimating the possibility of credit default or financial instability [1, 3]. Healthcare applications, on the other hand, deal with highly sensitive patient data such as demographics, clinical diagnoses, laboratory measurements, admission histories, and treatment records, necessitating predictive models capable of identifying patients at high clinical or operational risk. Urban planning becomes increasingly challenging as environmental monitoring systems continuously gather spatial and

temporal observations from distributed sensing stations, creating dynamic data streams that change in response to weather conditions, seasonal variations, traffic patterns, and human activities. The significant disparities in feature distributions, temporal dynamics, and prediction objectives make developing a unified risk forecasting system very difficult [3, 4].

Conventionally, machine learning models for risk forecasting are created using centralized training paradigms, in which data obtained from various businesses is consolidated into a single repository prior to model construction. Although centralized learning frequently produces high prediction results, it implies unlimited access to raw data, which is becoming increasingly difficult in practice [4, 5]. Financial firms are bound by rigorous regulatory requirements and confidentiality agreements, healthcare services must adhere to patient privacy restrictions, and public bodies responsible for urban sensing infrastructures frequently face legal and organizational impediments that hinder data sharing. These privacy, ownership, and governance constraints significantly limit the possibility of centralized data integration, highlighting the need for collaborative learning systems that may use distributed datasets without disclosing sensitive information [5, 6].

Federated learning (FL) has emerged as a successful paradigm for distributed model training in privacy-preserving situations, allowing numerous participants to collaborate on optimizing a shared model while maintaining raw data locally. Rather than sending sensitive observations to a central server, participating clients exchange model parameters or gradients, lowering privacy concerns and data transit. Due to these benefits, federated learning has been successfully examined in a variety of application fields, including financial fraud detection, healthcare analytics, intelligent transportation, mobile computing, and industrial Internet of Things [3, 6]. Nonetheless, most contemporary federated learning algorithms are based on the premise that participating client's complete identical prediction tasks with data from comparable distributions. In real-world configurations, nonetheless, enterprises frequently exhibit substantial variation in terms of data distributions, feature spaces, computational resources, and learning objectives, reducing the success rate of traditional aggregated data techniques such as Federated Averaging (FedAvg) [7, 8].

The problem becomes even more evident in cross-sector federated learning, because participants belong to wholly distinct application domains rather than different organizations within the same domain. Financial firms, hospitals, and urban monitoring organizations collect data with various statistical features and maximize separate prediction aims despite sharing the broader purpose of risk assessment. Directly aggregating local model parameters across such varied sectors may result in negative transfer, in which information obtained in one area has a negative impact on performance in another. Recent research on heterogeneous and customized federated learning has shown that tackling statistical heterogeneity necessitates learning algorithms that may preserve common knowledge while also adjusting to domain-specific properties. However, most present techniques focus on homogenous application situations, with very little attention paid to unified federated risk forecasting across several diverse industries [9, 10].

2. Related Work

2.1 Financial Risk Forecasting

Financial risk forecasting has become a key component of modern banking and financial management, allowing firms to predict probable credit defaults, loan delinquencies, and investment hazards before they result in severe financial losses. Traditional statistical methods, such as logistic regression and survival analysis, have steadily been complemented by machine learning algorithms capable of modelling complex nonlinear connections in high-dimensional financial data [2]. Decision trees, random forests, gradient boosting algorithms, support vector machines, and deep neural networks have all demonstrated superior predictive performance by incorporating customer demographics, credit history, income characteristics, repayment behaviour, and transactional data into comprehensive risk assessment models. These data-driven approaches have considerably improved credit scoring systems' accuracy and robustness, while minimizing the need for manual intervention in financial decisions [3].

Recent improvements have centred on deep learning architectures that automatically learn latent feature representations from diverse financial datasets. Neural networks that incorporate attention mechanisms, residual learning, and transformer-based topologies have demonstrated promising performance in credit risk analysis because they capture complicated relationships between financial indicators more well than traditional machine learning models. Nonetheless, the majority of extant research presume centralized access to consumer data collected from various branches or institutions, which limits their application in real-world financial systems where regulatory and privacy constraints frequently prevent direct data sharing. As a result, privacy-preserving collaborative learning has become a more essential direction for financial risk analytics [9, 28].

2.2 Healthcare Risk Prediction

Electronic health records, laboratory investigations, clinical diagnoses, medical imaging, wearable devices, and hospital information systems all contribute to the ongoing generation of vast amounts of patient data. These many data sources have aided in the creation of predictive models for disease diagnosis, hospital readmission, patient deterioration, mortality prediction, extended hospitalization, and resource allocation [10, 15 – 17, 20, 21]. Recent machine learning methods use ensemble learning, recurrent neural networks, graph neural networks, and transformer topologies to simulate complicated clinical linkages and temporal interactions in patient records [16, 20, 25, 29].

Despite these advancements, healthcare data remains one of the most sensitive types of personal information, making centralized model creation more difficult due to rigorous privacy restrictions and institutional governance norms [10, 15 – 17, 20, 21, 25]. Federated learning has gained a lot of interest as an excellent approach for collaborative healthcare analytics since it allows participating hospitals to build predictive models without transferring patient-level data. However, clinical institutions usually differ in terms of patient demographics, disease incidence, medical equipment, and treatment regimens, resulting in highly heterogeneous data distributions that can decrease the efficiency of traditional federated aggregation algorithms. Personalized federated learning algorithms have so emerged as a possible avenue for increasing predictive performance while maintaining institutional privacy [10, 15, 16, 20, 21].

2.3 Urban Risk Forecasting

The fast implementation of smart city infrastructures has allowed for continuous monitoring of environmental variables via regionally distributed sensing networks. Air-quality monitoring stations, traffic sensors, meteorological systems, and Internet of Things (IoT) devices create large-scale spatiotemporal data that aids in intelligent urban management. These metrics are increasingly being utilized to forecast pollution incidents, transportation congestion, environmental dangers, and infrastructure breakdowns [1].

Compared to traditional tabular datasets, urban sensing data show significant temporal volatility, geographical correlation, seasonality, and concept drift due to weather conditions, human activities, and traffic patterns [4]. Several studies have looked into recurrent neural networks, long short-term memory networks, temporal convolutional networks, graph neural networks, and transformer-based forecasting models to capture these complex dependencies [9]. Although these algorithms attain competitive forecast accuracy in centralized settings, practical urban monitoring systems frequently involve many agencies and geographically spread sensing infrastructures, making it difficult to aggregate raw observations into a single repository [11, 12].

2.4 Federated Learning and Personalized Federated Learning

Federated learning is a distributed machine learning approach that allows numerous organizations or devices to train a common model while keeping raw data local. Instead of transmitting sensitive observations to a centralized server, participating clients exchange only model updates, lowering privacy concerns and communication costs [1, 9]. Since the advent of the Federated Averaging (FedAvg) algorithm, federated learning has gained popularity in banking, healthcare, industrial IoT, mobile computing, and smart city applications [1, 4, 9].

However, statistical heterogeneity, system heterogeneity, communication restrictions, and model heterogeneity all hinder federated learning deployment in practice [1, 9]. Conventional FedAvg implies that participating clients have identical data distributions and learning objectives, which is rarely true in real-world implementations. Recent surveys have found that heterogeneous federated learning remains one of the most significant open challenges in distributed artificial intelligence, motivating the development of personalized federated learning, model-heterogeneous federated learning, and federated transfer learning to better accommodate diverse client characteristics [5, 9, 11, 12]. Personalized techniques often mix globally shared knowledge with client-specific model components, allowing each participant to adjust to local data while still receiving collaborative training [5, 8].

2.5 Cross-Sector Federated Risk Forecasting

Although federated learning has been extensively studied inside distinct application domains, there has been very little emphasis paid to collaborative learning across fundamentally different sectors. Existing federated learning experiments are often conducted in homogeneous contexts with clients from the same application domain, such as several hospitals, financial institutions, or mobile devices [10, 15 – 21]. In contrast, cross-sector federated learning necessitates collaborative optimization across domains with different feature spaces, statistical characteristics, temporal dynamics, and prediction goals. Such

heterogeneity significantly raises the probability of negative transfer, which occurs when information useful to one domain has a harmful effect on learning in another.

Recent research in heterogeneous and customized federated learning has offered adaptive aggregation algorithms, client-specific model components, knowledge distillation, and transfer learning mechanisms to deal with statistical and architectural heterogeneity [5, 11, 12]. Nonetheless, most available approaches have been tested on homogeneous benchmark datasets rather than in real-world multi-sector scenarios. Furthermore, few studies have looked into unified risk forecasting frameworks that can support financial, healthcare, and urban planning tasks all at once using a shared privacy-preserving federated learning framework [6, 7, 13, 14, 22]. This constraint inspired the creation of the proposed personalized cross-sector federated learning architecture, which blends shared knowledge learning and sector-specific adaptation to increase prediction performance across many domains [5, 8].

3. Proposed Methodology

This paper provides a personalized cross-sector federated learning framework for risk forecasting in three different domains: finance, healthcare, and urban planning. The approach is intended to teach transferable risk representations without explicitly sharing actual sectoral data. Unlike traditional federated learning, which trains a single global model for all participants, the proposed method divides the network into shared and sector-specific components. The shared component captures common predictive patterns across sectors, whereas personalized components tailor the learnt representation to the specific characteristics of each sector.

The proposed framework consists of five major components: sector-specific data preprocessing, a shared gated residual encoder, sector-conditioned feature modulation, private residual adapters and prediction heads, and equal-sector federated aggregation using FedProx regularization. Figure 1 depicts the total workflow for the proposed design.

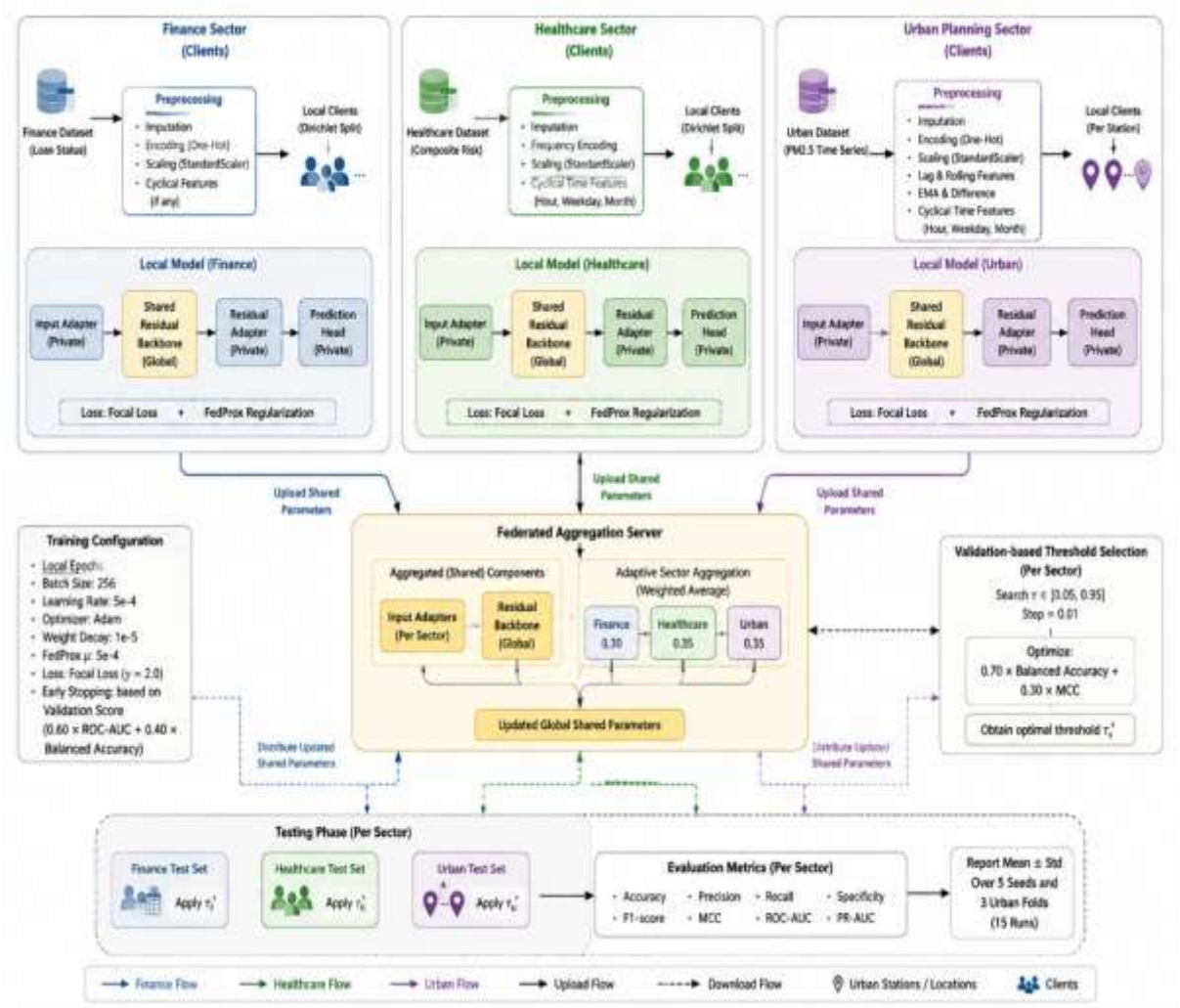

Figure 1. Proposed personalized federated learning framework for cross-sector risk forecasting across finance, healthcare, and urban planning.

3.1 Cross-Sector Problem Formulation

Let the participating sectors be represented by

$$\mathcal{S} = \{\mathcal{S}_f, \mathcal{S}_h, \mathcal{S}_u\},$$

where $\mathcal{S}_f$, $\mathcal{S}_h$, and $\mathcal{S}_u$denote the finance, healthcare, and urban-planning sectors, respectively. Each sector possesses a local dataset

$$\mathcal{D}_s = \{(x_i^s, y_i^s)\}_{i=1}^{N_s},$$

where $x_i^s \in \mathbb{R}^{d_s}$denotes the input feature vector, $y_i^s \in \{0,1\}$represents the associated risk label, $d_s$is the original feature dimension, and $N_s$is the number of observations available in sector s.

Although every sector can use binary risk forecasting, their features and target definitions differ. The financial industry predicts the likelihood of financial default or credit-related risk, the healthcare sector identifies patients at high clinical risk, and the urban sector forecasts hazardous environmental or operational situations. As a result, directly training one identical model across all sectors may suppress sector-specific knowledge and cause negative transfer.

The objective is to learn a set of shared model parameters $\boldsymbol{\theta}$and sector-specific parameters $\boldsymbol{\phi}_s$by minimizing

$$\min_{\boldsymbol{\theta},\{\boldsymbol{\phi}_s\}} \frac{1}{|\mathcal{S}|} \sum_{s\in\mathcal{S}} \mathcal{L}_s(\boldsymbol{\theta}, \boldsymbol{\phi}_s; \mathcal{D}_s),$$

where $\mathcal{L}_s$ denotes the local prediction loss for sector s. The shared parameters are collaboratively updated through federated aggregation, whereas the personalized parameters remain specific to each sector.

3.2 Sector-Specific Data Preparation

The three datasets have distinct feature architectures, statistical distributions, and temporal characteristics. As a result, not all sectors are subject to the same preprocessing technique. Instead, each dataset is analyzed locally utilizing a sector-sensitive pipeline before being combined into a single latent input dimension.

3.2.1 Financial-Sector Preprocessing

The financial dataset includes numerical and categorical features about client characteristics, financial history, account information, and repayment behaviour. Missing numerical values are substituted with statistics estimated from the training partition, and categorical variables are encoded using an appropriate categorical encoding method. Continuous variables are normalized so that features with vast numerical ranges do not dominate model optimization.

The target variable indicates the presence or absence of financial risk. Data partitioning is done via stratified sampling, which preserves class proportions in the training, validation, and testing sets.

3.2.2 Healthcare-Sector Preprocessing

The healthcare dataset includes patient-specific variables such as demographics, clinical measures, diagnoses, admission features, and treatment-related aspects. Missing values and categorical variables are addressed with statistics and encoders that are only trained on training data.

To avoid target leakage, any threshold used to construct the healthcare risk label is derived entirely from the training partition. The same threshold is then applied to the validation and testing partitions. This approach assures that information from evaluation data is not used to influence target construction or model development.

3.2.3 Urban-Sector Preprocessing

The urban dataset is made up of time-indexed environmental or sensor observations. Because random splitting may allow future observations to impact model training, the urban sector is examined using a sequential or rolling temporal protocol. Earlier observations are utilized for training, followed by validation, and finally by testing.

Temporal characteristics, such as hour, day, month, and seasonal indications, can be retrieved when accessible. Continuous sensor data are scaled using parameters estimated during the training phase. This temporally ordered architecture enables a more accurate assessment of future risk projection.

3.2.4 Common Representation Dimension

After sector-specific preprocessing, the resulting input dimensions may differ substantially. Each sector therefore uses a local input projection layer:

$$\boldsymbol{z}_i^s = \sigma(\boldsymbol{W}_{in}^s \boldsymbol{x}_i^s + \boldsymbol{b}_{in}^s),$$

where $\boldsymbol{W}_{in}^s$and $\boldsymbol{b}_{in}^s$are sector-specific projection parameters, and $\sigma(\cdot)$denotes a nonlinear activation function. The projection maps the original input into a common latent dimension d, enabling the sectors to use the same shared encoder despite their different original feature spaces.

The input projection remains local because its parameters depend directly on the meaning and dimensionality of the sector-specific features.

3.3 Shared Gated Residual Encoder

The central component of the proposed architecture is a shared gated residual encoder. Its purpose is to learn transferable patterns that are useful across the participating sectors while maintaining stable gradient propagation during training.

Let z^s denote the projected input representation of sector s. A residual transformation is first calculated as

$$r^s = f_{res}(z^s; \theta_r),$$

where $f_{res}(\cdot)$ contains fully connected transformations, normalization, nonlinear activation, and dropout operations.

A gating vector is then generated by

$$g^s = sigmoid\left(W_g z^s + b_g\right).$$

The gated residual representation is obtained as

$$h^s = z^s + g^s \odot r^s,$$

where $\odot$ represents element-wise multiplication.

The gating mechanism determines how much transformed information should be incorporated into each latent feature. When a transformed feature is beneficial, the corresponding gate approaches one; otherwise, the original representation is largely preserved through the residual connection. This design reduces the likelihood that aggressively shared transformations will remove useful sector-specific information.

Multiple gated residual blocks can be stacked to form the shared encoder:

$$h_l^s = h_{l-1}^s + g_l^s \odot f_l(h_{l-1}^s),$$

where l denotes the block index. The parameters of these blocks are shared and aggregated across all sectors.

3.4 Sector-Conditioned Feature Modulation

Although the shared encoder learns similar representations, the importance of each latent feature may vary across domains. A depiction useful for financial risk may not be as relevant for clinical or urban risk. As a result, the suggested architecture applies feature modulation conditioned by sector.

For each sector s, two learnable vectors are maintained: a scaling vector $\gamma_s$and a shifting vector β_s. The shared representation is modulated as

$$\tilde{h}^s = \gamma_s \odot h^s + \beta_s.$$

The scaling vector determines the relevance of individual latent characteristics, whereas the shifting vector modulates their sector-specific activation levels. These parameters are local and not averaged across sectors.

Sector-conditioned modulation enables lightweight customisation without the need for a separate encoder for each sector. As a result, collaborative knowledge exchange is preserved, yet the same worldwide representation can be perceived differently by finance, healthcare, and urban clients.

3.5 Bottleneck Residual Adapters

After feature modulation, each sector uses a private bottleneck residual adapter. The adaptor learns a compact sector-specific transformation while adding only a few parameters to the overall model.

For sector s, the adapter is defined as

$$\boldsymbol{a}^s = \boldsymbol{W}_{up}^s \, \sigma\left(\boldsymbol{W}_{down}^s \tilde{\boldsymbol{h}}^s + \boldsymbol{b}_{down}^s\right) + \boldsymbol{b}_{up}^s,$$

where $\boldsymbol{W}_{down}^s$reduces the representation to a lower-dimensional bottleneck, and $\boldsymbol{W}_{up}^s$projects it back to the original latent dimension.

The personalized output is calculated using a residual connection:

$$\boldsymbol{p}^s = \tilde{\boldsymbol{h}}^s + \boldsymbol{a}^s.$$

The bottleneck structure restricts the amount of individualized parameters and reduces overfitting, especially in sectors with small datasets. The residual link also ensures that the sector has access to the shared representation even if the adapter transformation is not useful.

3.6 Sector-Specific Prediction Heads

Each sector uses a private nonlinear prediction head to map the personalized representation to its corresponding risk probability. The head is defined as

$$\boldsymbol{q}^s = \sigma(\boldsymbol{W}_1^s \boldsymbol{p}^s + \boldsymbol{b}_1^s),$$

followed by

$$o^s = \boldsymbol{W}_2^s \boldsymbol{q}^s + b_2^s,$$

where $o^s$is the output logit. The predicted probability of risk is obtained through the sigmoid function:

$$\hat{y}^s = \frac{1}{1 + exp(-o^s)}.$$

The use of sector-specific heads is necessary because the interpretation of the positive risk class differs across domains. A financial-risk prediction represents a different event from a healthcare or urban-risk prediction, even when all tasks are formulated as binary classification.

3.7 Balanced Focal Loss

Cross-sector risk datasets commonly exhibit class imbalance, with high-risk observations occurring less frequently than normal observations. Standard binary cross-entropy may therefore cause the model to prioritize the majority class.

To reduce this problem, the proposed framework employs a balanced focal loss:

$$\mathcal{L}_{focal} = -\alpha y(1-\hat{y})^{\gamma} log(\hat{y}) - (1-\alpha)(1-y)\hat{y}^{\gamma} log(1-\hat{y}),$$

where αcontrols class weighting and γdetermines the degree to which easy observations are down-weighted.

The modulating factors $(1-\hat{y})^{\gamma}$and $\hat{y}^{\gamma}$reduce the contribution of correctly classified observations and place greater emphasis on difficult or minority-class cases. This is particularly important for risk forecasting, where failure to identify a high-risk observation may have substantial operational consequences.

3.8 FedProx-Based Local Optimization

The varied distributions of the participating sectors can lead the locally trained shared parameters to move in significantly divergent directions. This process, known as client drift, can make global aggregation unstable.

To reduce local divergence, the proposed framework includes a FedProx regularization term in the sector-level objective:

$$\mathcal{L}_s^{prox} = \mathcal{L}_s^{focal} + \frac{\mu}{2} \parallel \boldsymbol{\theta}_s - \boldsymbol{\theta}^{(t)} \parallel_2^2,$$

where θ_s denotes the locally updated shared parameters, $\theta^{(t)}$denotes the global shared parameters at communication round t, and $\mu$is the proximal regularization coefficient.

The proximate term prohibits each sector from migrating too far away from its current global representation. It does not, however, limit the sector-specific projection layers, modulation settings, adapters, or prediction heads because these components are purposefully customized.

3.9 Equal-Sector Federated Aggregation

Standard FedAvg weights each client update according to the number of local training observations:

$$\boldsymbol{\theta}^{(t+1)} = \sum_{s \in \mathcal{S}} \frac{N_s}{\sum_{j \in \mathcal{S}} N_j} \boldsymbol{\theta}_s^{(t+1)}.$$

Although this approach is suitable when clients represent comparable partitions of the same domain, it may be inappropriate for cross-sector learning. A sector with a substantially larger dataset can dominate the shared encoder, even though all sectors are equally important to the study.

The proposed framework therefore applies equal-sector aggregation:

$$\boldsymbol{\theta}^{(t+1)} = \frac{1}{\mid \mathcal{S} \mid} \sum_{s \in \mathcal{S}} \boldsymbol{\theta}_s^{(t+1)}.$$

With three sectors, each sector contributes one-third of the aggregated shared update, regardless of its sample size. Only the shared encoder parameters are aggregated. The following parameters remain private:

$$\boldsymbol{\phi_s} = \{\boldsymbol{W_{in}^s}, \boldsymbol{\gamma_s}, \boldsymbol{\beta_s}, \boldsymbol{W_{down}^s}, \boldsymbol{W_{up}^s}, \boldsymbol{W_1^s}, \boldsymbol{W_2^s}\}.$$

This separation prevents incompatible feature projections and task-specific classifiers from being averaged across unrelated sectors.

3.10 Federated Training Procedure

At the beginning of communication round t, the server distributes the current shared encoder parameters $\boldsymbol{\theta}^{(t)}$to all participating sectors. Each sector combines the received parameters with its private projection, modulation, adapter, and prediction-head parameters.

Local training is then carried out for a predetermined number of epochs, utilizing the sector's training data. During local optimization, the shared and personalized parameters are updated simultaneously with the balanced focal loss and FedProx regularization. Following local training, each sector sends just the modified shared encoder settings to the server.

The server computes the next global shared model using equal-sector aggregation. The aggregated parameters are reallocated for the subsequent communication round. This method is repeated until the maximum number of rounds is achieved or the validation performance stops improving.

The entire training procedure is given in Algorithm 1.

Algorithm 1: Personalized Cross-Sector Federated Training

Input: Sector datasets $\{\mathcal{D}_s\}_{s=1}^{S}$, number of rounds T, local epochs E, learning rate η, and proximal coefficient μ.

Output: Global shared parameters $\boldsymbol{\theta}^*$and personalized sector parameters $\{\boldsymbol{\phi}_s^*\}_{s=1}^{S}$.

1. Initialize the global shared encoder parameters $\boldsymbol{\theta}^{(0)}$.
2. Initialize the personalized parameters $\boldsymbol{\phi}_s^{(0)}$for every sector.

3. For each communication round $t = 0,1, \ldots, T-1$:
    1. Distribute $\boldsymbol{\theta}^{(t)}$ to all participating sectors.
    2. For each sector s:
        1. Set the local shared parameters to $\boldsymbol{\theta}^{(t)}$.
        2. Train the local model for E epochs.
        3. Minimize the focal prediction loss and FedProx regularization term.
        4. Retain the updated private parameters $\boldsymbol{\phi}_s^{(t+1)}$ locally.
        5. Transmit only the updated shared parameters $\boldsymbol{\theta}_s^{(t+1)}$.
    3. Aggregate the received parameters using

$$\boldsymbol{\theta}^{(t+1)} = \frac{1}{S}\sum_{s=1}^{S} \boldsymbol{\theta}_s^{(t+1)}.$$

    4. Evaluate the personalized sector models on their validation sets.
    5. Apply early stopping when the validation criterion does not improve for a predefined patience period.
4. Restore the best-performing shared and personalized parameters.

3.11 Experimental Workflow

The entire experimental workflow used to assess the suggested Personalized FedProx framework is shown in Figure 2. The first step in the process is gathering diverse datasets from the urban, healthcare, and financial sectors. Sector-specific preprocessing is applied to each dataset, such as temporal feature engineering for the urban dataset, feature encoding, feature scaling, and missing-value imputation. Non-IID client generation techniques are then used to divide the processed data into several federated clients. For example, Dirichlet-based partitioning is used to divide healthcare and financial data, while monitoring stations are used to group urban data.

Using the FedProx optimization technique, each client builds a customized local model with sector-specific input adapters, a shared residual backbone, private residual adapters, and task-specific prediction heads. Only the shared backbone parameters are sent to the central server following local training, where adaptive sector-weighted aggregation maintains sector-specific components while updating the global model. All participating clients then receive the updated shared backbone, and this communication process is repeated until convergence.

Following model training, validation data are used to determine the optimal decision threshold independently for each sector. The optimized models are then evaluated on the corresponding test sets using Accuracy, Balanced Accuracy, Precision, Recall, Specificity, F1-score, Matthews Correlation Coefficient (MCC), ROC-AUC, and PR-AUC. To ensure robustness and reproducibility, the complete evaluation is repeated using five random seeds and three rolling temporal folds for the urban dataset, resulting in 15 experimental runs from which the mean and standard deviation of each performance metric are reported.

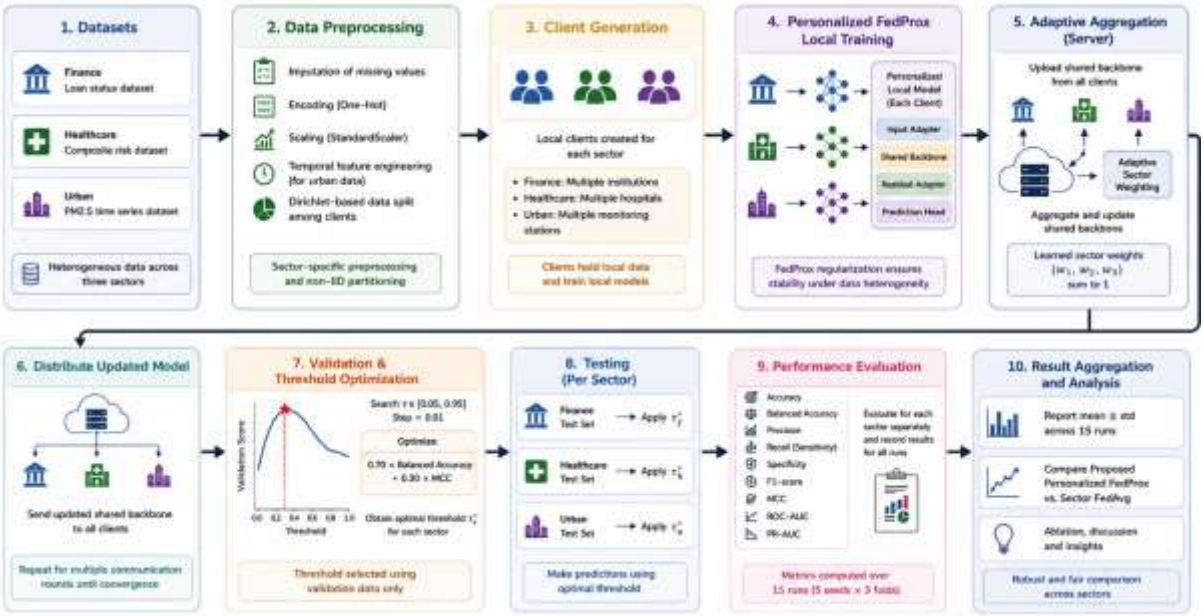

Figure 2. Experimental workflow of the proposed Personalized FedProx framework.

3.12 Validation-Based Decision-Threshold Selection

A fixed decision threshold of 0.5may be unsuitable when sectors exhibit different class distributions and misclassification patterns. Therefore, an independent threshold is selected for each sector using only its validation partition.

The candidate threshold set is defined as

$$\mathcal{T} = \{0.05, 0.055, \dots, 0.95\}.$$

For each candidate threshold τ, the validation score is computed as

$$J_s(\tau) = 0.50F_{1,s}(\tau) + 0.30BAcc_s(\tau) + 0.20MCC_s(\tau),$$

where $F_{1,s}$, $BAcc_s$, and MCC_sdenote the F1-score, balanced accuracy, and Matthews correlation coefficient for sector s, respectively.

The optimal sector-specific threshold is selected as

$$\tau_s^* = arg\ max\ \tau \in T\ J_s(\tau).$$

The final prediction is calculated as

$$\hat{c}_i^s = \begin{cases} 1, & \hat{y}_i^s \geq \tau_s^*, \\ 0, & \hat{y}_i^s < \tau_s^*. \end{cases}$$

The selected threshold is applied unchanged to the corresponding test set, and no test-set information is used during threshold selection.

3.13 Repeated Experimental Evaluation

To reduce the influence of random initialization and stochastic optimization, each experiment is repeated using multiple random seeds. For an evaluation metric M, the mean result is calculated as

$$\bar{M} = \frac{1}{R}\sum_{r=1}^{R} M_r\,,$$

where $R$is the number of repeated runs. The standard deviation is calculated as

$$\sigma_M = \sqrt{\frac{1}{R-1}\sum_{r=1}^{R}(M_r - \bar{M})^2}\,.$$

The results are reported as

$$\bar{M} \pm \sigma_M.$$

This evaluation procedure provides a more reliable assessment than reporting the result of a single experimental run.

4. Results and Discussion

4.1 Experimental Setup

Three publicly accessible datasets covering diverse application domains; finance, healthcare, and urban planning—were used to assess the suggested Personalized FedProx framework. The urban dataset was utilized for next-hour environmental risk forecasting, the healthcare dataset for patient risk prediction, and the finance dataset for binary credit-risk prediction. While sector-specific preprocessing and target generation were carried out locally, the same preprocessing approach, model architecture, and evaluation protocol were used across all sectors to guarantee a fair comparison.

Each experiment was repeated with five random seeds to lessen the impact of random initialization and stochastic optimization. In order to maintain the chronological order of the data and avoid information leakage from subsequent observations into the training process, a rolling temporal evaluation with three sequential folds was used because the urban dataset contains temporal observations. As a result, 15 separate experimental runs were used to analyze each method–sector combination. The final results are shown as the mean ± standard deviation of the corresponding evaluation metrics.

The PyTorch deep learning framework was used to implement each experiment in Python. A workstation with an Intel Core i7 processor, 16 GB RAM, and an NVIDIA GeForce GTX 1660 Ti Max-Q GPU (6 GB VRAM) with CUDA acceleration was used for model training. The Adam optimizer with balanced focal loss and FedProx regularization was used to train the Personalized FedProx framework. Adaptive sector-weighted aggregation was used to update the shared residual backbone between communication rounds.

Several performance metrics, such as Accuracy, Balanced Accuracy, Precision, Recall, Specificity, F1-score, Matthews Correlation Coefficient (MCC), Receiver Operating Characteristic Area Under the Curve (ROC-

AUC), and Precision–Recall Area Under the Curve (PR-AUC), were used to compare the suggested framework with the Sector FedAvg baseline. To assess the resilience and discriminative power of the suggested framework across the three application areas, confusion matrices, ROC curves, and repeated-run performance statistics were examined in addition to quantitative performance comparison.

4.2 Federated Training Convergence

The convergence behavior of the Sector FedAvg baseline and the suggested Personalized FedProx framework during federated training is shown in Figure 3. Both approaches quickly increase their validation performance during early communication rounds, suggesting that collaborative learning successfully captures transferable representations across three application domains. The rate of progress slows down when both models get closer to convergence around the tenth communication round. Nevertheless, the suggested framework keeps showing steady improvements in performance and eventually reaches a better validation score (about 0.655) than Sector FedAvg (around 0.644). Combining sector-specific personalization with FedProx regularization stabilizes optimization under heterogeneous data distributions, as seen by the smoother convergence trend and decreased performance fluctuations. These results imply that the suggested approach retains domain-specific information through private model components while learning more generalized common representations.

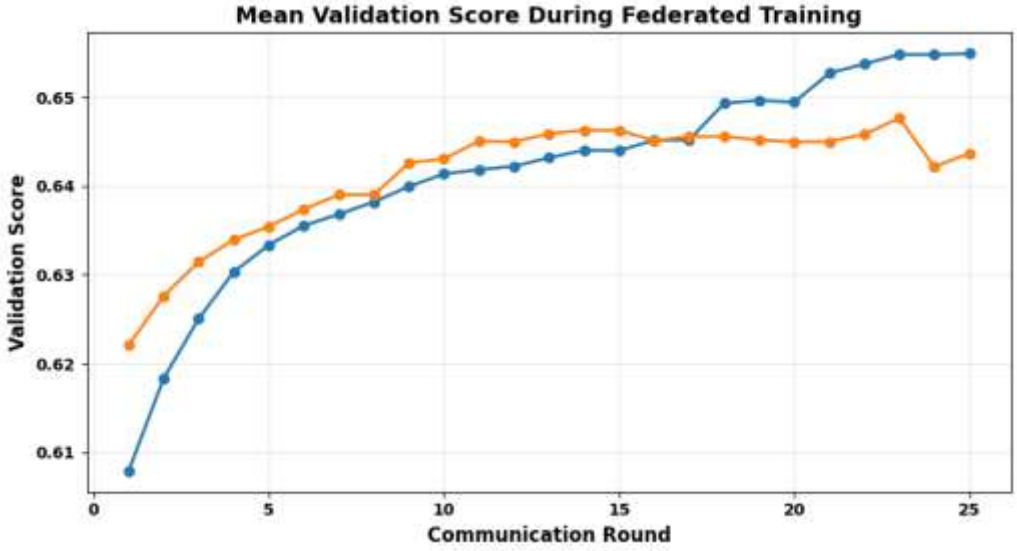

Figure 3. Mean validation score during federated training over 25 communication rounds.

4.3 Experimental Performance Overview

The proposed personalized cross-sector federated learning system was compared to Sector FedAvg for banking, healthcare, and urban risk forecasting tasks. Each approach was evaluated using five random seeds and three rolling urban folds, yielding 15 experimental runs for each method-sector combination. The performance was assessed using accuracy, balanced accuracy, precision, recall, specificity, F1-score, Matthew's correlation coefficient, ROC-AUC, and PR-AUC.

Table 1 shows the mean ± SD of the proposed Personalized FedProx framework and Sector FedAvg across 15 trial runs. Overall, the proposed strategy delivered competitive results in all three areas. In the finance industry, both techniques yielded similar results, with the proposed framework exhibiting small gains in accuracy, MCC, ROC-AUC, and PR-AUC. In healthcare, the suggested strategy enhanced overall accuracy while maintaining similar balanced accuracy, ROC-AUC, and PR-AUC to the baseline, indicating that the prediction task remained tough. The most significant benefits were seen in the urban area, where the suggested framework consistently outperformed all assessment criteria, particularly ROC-AUC and PR-AUC. These findings indicate that the personalized design efficiently protects sector-specific traits while using cross-sector collaborative learning.

Table 1. Mean ± standard deviation results across 15 runs.

Method	Sector	Accuracy	Balanced Accuracy	F1-score	MCC	ROC-AUC	PR-AUC
Proposed Personalized FedProx	Finance	**0.8893 ± 0.0172**	0.8193 ± 0.0108	0.7341 ± 0.0287	**0.6681 ± 0.0432**	**0.9027 ± 0.0091**	**0.8178 ± 0.0240**

Proposed Personalized FedProx	Healthcare	**0.5686 ± 0.0579**	0.5017 ± 0.0038	0.2729 ± 0.1431	**0.0053 ± 0.0108**	0.5017 ± 0.0043	0.3509 ± 0.0048
Proposed Personalized FedProx	Urban	**0.5430 ± 0.0966**	**0.5707 ± 0.0414**	**0.5064 ± 0.0621**	**0.1559 ± 0.0708**	**0.6227 ± 0.0360**	**0.4872 ± 0.0460**
Sector FedAvg	Finance	0.8871 ± 0.0265	**0.8229 ± 0.0183**	**0.7355 ± 0.0436**	0.6668 ± 0.0624	0.9014 ± 0.0167	0.8164 ± 0.0457
Sector FedAvg	Healthcare	0.5257 ± 0.0977	**0.5032 ± 0.0046**	**0.3128 ± 0.1919**	0.0051 ± 0.0138	**0.5030 ± 0.0044**	**0.3515 ± 0.0047**
Sector FedAvg	Urban	0.5383 ± 0.0976	0.5659 ± 0.0539	0.5045 ± 0.1049	0.1404 ± 0.0922	0.6017 ± 0.0566	0.4567 ± 0.0662

Table 2 summarizes the performance improvement of the proposed framework over Sector FedAvg across 15 runs. The greatest improvement was shown in healthcare accuracy (+0.0429), but advances in other healthcare indicators were restricted, showing that higher accuracy did not result in significantly better class discrimination. In the finance industry, the mean improvements were small, indicating that both techniques produced almost comparable results. The urban sector showed the most consistent increases, especially in ROC-AUC (+0.0211) and PR-AUC (+0.0305), with the suggested framework outperforming the baseline in 60% and 73.33% of runs, respectively. Overall, the findings show that the proposed Personalized FedProx framework provides sector-specific enhancements, with the highest impact for urban risk forecasting while preserving competitiveness in banking and healthcare.

Table 2. Performance gain of the proposed method over Sector FedAvg across 15 runs.

Metric	Sector	Mean Gain	Standard Deviation of Gain	Positive Runs (%)
Accuracy	Finance	+0.0022	0.0326	53.33
Accuracy	Healthcare	**+0.0429**	0.0737	**73.33**
Accuracy	Urban	+0.0047	0.0892	46.67
Balanced Accuracy	Finance	−0.0036	0.0212	33.33
Balanced Accuracy	Healthcare	−0.0016	0.0051	40.00
Balanced Accuracy	Urban	+0.0048	0.0484	53.33
F1-score	Finance	−0.0013	0.0535	46.67
F1-score	Healthcare	−0.0399	0.1269	26.67
F1-score	Urban	+0.0019	0.0882	33.33
MCC	Finance	+0.0012	0.0779	53.33
MCC	Healthcare	+0.0002	0.0174	46.67
MCC	Urban	+0.0155	0.0776	46.67
ROC-AUC	Finance	+0.0013	0.0189	40.00
ROC-AUC	Healthcare	−0.0013	0.0059	33.33
ROC-AUC	Urban	**+0.0211**	0.0592	60.00
PR-AUC	Finance	+0.0014	0.0532	40.00
PR-AUC	Healthcare	−0.0006	0.0051	40.00
PR-AUC	Urban	**+0.0305**	0.0505	**73.33**

The mean performance boost attained by the suggested Personalized FedProx framework over Sector FedAvg across the three application domains is shown graphically in Figure 4. With gains remaining near zero for all evaluation parameters, the finance sector shows very slight variations between the two approaches, suggesting similar predictive performance. The healthcare industry, on the other hand, exhibits the most improvement in overall accuracy (+0.043). However, negative gains in Balanced Accuracy, F1-score, ROC-AUC, and PR-AUC indicate that the rise in accuracy did not correlate with stronger class discrimination. All evaluation metrics show positive growth in the urban sector, with MCC (+0.015), ROC-AUC (+0.021), and PR-AUC (+0.030) showing the most consistent improvements. These results show that the suggested personalized federated learning architecture maintains competitive performance in the financial and healthcare industries while being particularly successful for temporally developing urban-risk prediction.

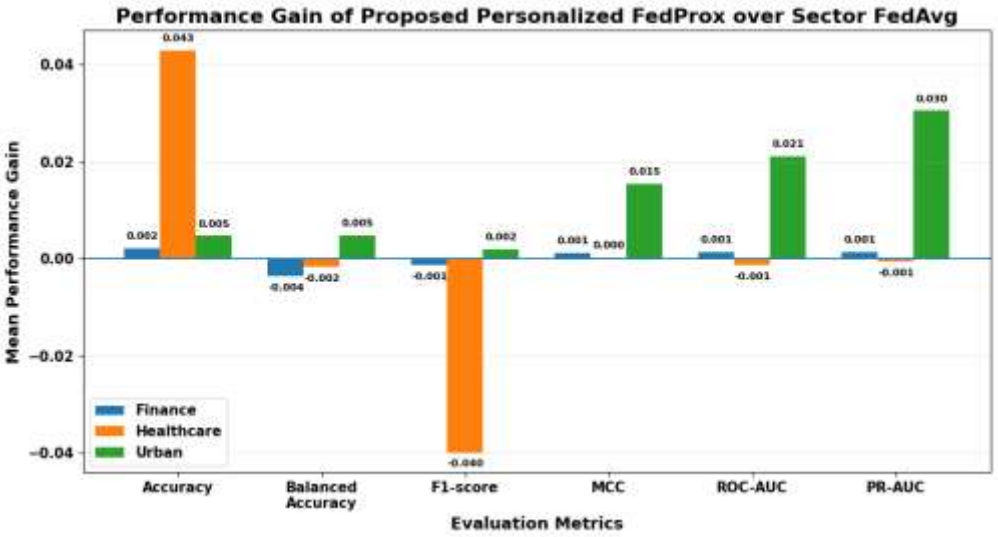

Figure 4. Mean performance gain of the proposed Personalized FedProx framework over Sector FedAvg across finance, healthcare, and urban sectors.

4.4 Financial Risk Forecasting Results

The financial sector had the best overall performance of the three application domains. The suggested Personalized FedProx approach had an accuracy of 0.8893±0.0172, balanced accuracy of 0.8193±0.0108, F1-score of 0.7341±0.0287, MCC of 0.6681±0.0432, ROC-AUC of 0.9027±0.0091, and PR-AUC of 0.8178±0.0240.

These findings suggest that the financial objective includes adequately informative links between borrower attributes and the original loan-status target. The strong ROC-AUC indicates that the learnt model can effectively score hazardous and non-risky borrowers over a variety of thresholds. The relatively high PR-AUC is particularly noteworthy because only about 21.9% of the financial observations are positive, making the job moderately imbalanced.

Compared to Sector FedAvg, the proposed technique increased mean accuracy by 0.0022, MCC by 0.0012, ROC-AUC by 0.0013, and PR-AUC by 0.0014. However, its balanced accuracy dropped by 0.0036 and its F1-score fell by 0.0013.

These variations are relatively minor. As a result, the financial outcomes should not be interpreted as a decisive advantage of the proposed strategy. Instead, they propose that the personalized architecture-maintained performance comparable to the sector-specific baseline while allowing for cross-sector sharing. The most plausible view is that customization and FedProx prevented huge negative transfers but did not result in a significant predictive advantage for finance.

The positive-run percentages back up this cautious assessment. The suggested model improved financial accuracy in 53.3% of runs, MCC in 53.3%, ROC-AUC in 40%, and PR-AUC in 40%. Its balancing accuracy improved in just 33.3% of runs. Thus, the financial gains varied between seeds and folds.

4.5 Healthcare Risk Prediction Results

The proposed technique achieved a mean healthcare accuracy of 0.5686±0.0579, compared to 0.5257±0.0977 for Sector FedAvg. This translates into an average accuracy improvement of 0.0429, or about 4.29 percentage points. In 73.3% of the experimental runs, the proposed technique performed better than the baseline in terms of healthcare accuracy.

This is the most significant accuracy improvement among the three areas. The suggested model significantly lowered the variability of healthcare accuracy from 0.0977 under Sector FedAvg to 0.0579, demonstrating more consistent performance over multiple runs.

However, the remaining healthcare data indicate that the task was not learned adequately. The suggested framework achieved a balanced accuracy of 0.5017±0.0038, MCC of 0.0053±0.0108, and ROC-AUC of 0.5017±0.0043. These values are similar to random classification.

The F1-score was 0.2729±0.1431, lower than the Sector FedAvg of 0.0399 on average. The proposed strategy resulted in a higher healthcare F1-score in only 26.7% of runs. It also demonstrated modestly negative increases in balancing accuracy, ROC-AUC, and PR-AUC.

The rise in ordinary accuracy should not be taken as a general improvement in healthcare-risk discrimination. Because accuracy can improve with changes in the projected class distribution, it may mask

poor minority-class recognition. The model's capacity to identify high-resource-risk patients from lower-risk patients is restricted, as seen by a near-zero MCC and a ROC-AUC of 0.50.

The nature of the built target is one plausible explanation. The healthcare risk label is calculated using the length of stay, billing amount, and abnormal test status, but the direct target components are eliminated from the input features. This leakage-safe design is methodologically sound, but it presents a severe indirect prediction difficulty. The remaining demographic, admission, insurance, and clinical categorical factors may not provide enough predictive information to accurately rebuild the composite resource-risk score.

The substantial standard deviation of the healthcare F1-score suggests threshold instability. Despite the fact that ROC-AUC remains consistently near to 0.50, the threshold used for validation may result in very varied precision-recall trade-offs among random partitions. As a result, the healthcare data show that poor discrimination is more stable than excellent risk predicting.

4.6 Urban Risk Forecasting Results

The urban sector performed about averagely. The suggested technique achieved an accuracy of 0.5430±0.0966, balanced accuracy of 0.5707±0.0414, F1-score of 0.5064±0.0621, MCC of 0.1559±0.0708, ROC-AUC of 0.6227±0.0360, and PR-AUC of 0.4872±0.0460. The proposed framework outperformed Sector FedAvg on all six reported mean measures for the urban sector. Gains were Accuracy: +0.0047; balanced accuracy: +0.0048; F1-score: +0.0019; MCC: +0.0155; ROC-AUC: +0.0211; and PR-AUC: +0.0305. The proposed model had a higher urban ROC-AUC in 60% of runs and a higher PR-AUC in 73.3% of them.

The most significant improvements are in ROC-AUC and PR-AUC. The ROC-AUC increased from around 0.602 to 0.623, indicating that the shared residual backbone and sector-specific adaptor enhanced the ranking of next-hour PM2.5 increase occurrences. The PR-AUC improvement is especially significant because positive-class proportions differed across temporal folds.

The rolling folds show substantial shifts in class distribution. The test positive rates were around 38.8%, 29.9%, and 39.6% across the three folds, with learnt relative-change thresholds ranging from 0.0392 to 0.0440. This variation helps to explain the comparatively high standard deviation in urban accuracy.

The small MCC of 0.1559 and the balanced accuracy of 0.5707 indicate that the urban mission remains difficult. Predicting a significant next-hour PM2.5 increase is sensitive to abrupt local changes that may not be fully captured by past pollutant measurements alone. Although the constructed lag, rolling, exponential-moving-average, difference, and cyclical time elements add temporal context, the dataset only includes two monitoring stations and 1,341 useable observations. Generalization is limited by the confined spatial and temporal coverage.

Nonetheless, the urban outcomes provide the most compelling evidence that cross-sector tailored sharing may have some benefits. Unlike finance, where performance remained almost same, and healthcare, where discrimination remained random, the urban sector demonstrated persistent mean increases in all key indicators, particularly ranking-based measures.

Figure 5 shows the confusion matrices generated by the proposed Personalized FedProx framework for the three application domains. In the finance sector, the model successfully identified 4,629 lower-risk and 1,005 higher-risk occurrences, with just 436 false positives and 413 incorrect negatives. The balanced distribution of correctly categorized samples shows that the proposed framework efficiently distinguishes between low-risk and high-risk borrowers, which is supported by the high ROC-AUC presented in Table 1.

4.7 Confusion Matrix Analysis

The healthcare confusion matrix demonstrates a significant difference in behavior. The program accurately classified almost all lower-risk patients (7,154), but only five higher-risk cases, misclassifying 3,835 higher-risk patients as lower-risk. This explains the poor MCC and ROC-AUC values presented in Table 1, indicating that the healthcare prediction problem remains extremely difficult, despite improvements in overall accuracy. The substantial class imbalance and leakage-safe structure of the healthcare target all contribute to this conservative prediction behavior.

The confusion matrix in urban forecasting is more balanced than in healthcare. The suggested framework properly recognized 76 lower-risk and 47 higher-risk events, but incorrectly classified 46 lower-risk and 33 higher-risk observations. Although prediction errors persist, the model shows a good ability to discriminate future pollution-risk events, which supports the reported increases in balanced accuracy, ROC-AUC, and PR-AUC.

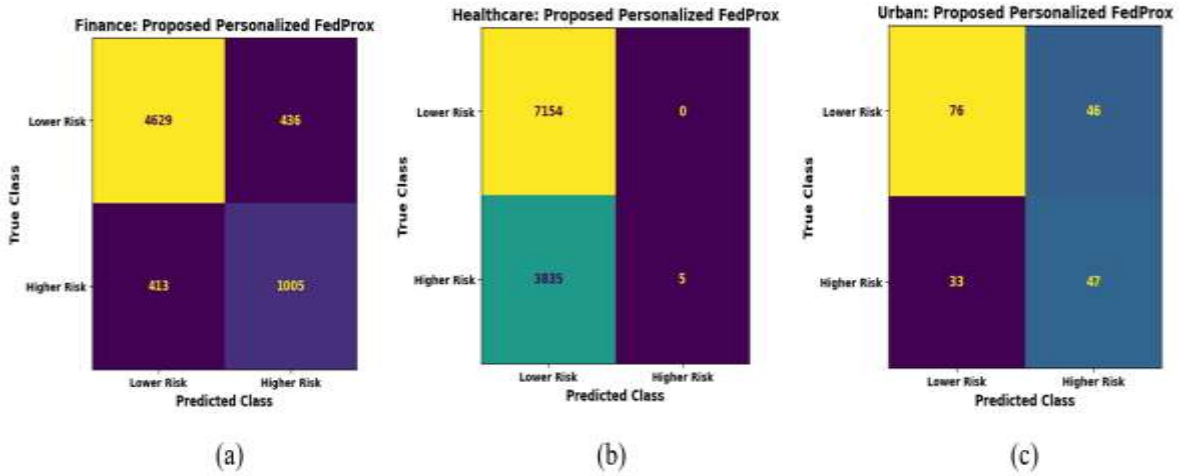

Figure 5. Confusion matrices of the proposed Personalized FedProx framework for (a) Finance, (b) Healthcare, and (c) Urban risk prediction.

4.8 ROC Curve Analysis

Figure 6 compares the ROC curves from the three application domains. The finance industry has the biggest area under the curve, showing strong discrimination between low-risk and high-risk borrowers at various decision thresholds. This observation is consistent with the ROC-AUC value of about 0.90 presented in Table X, indicating that the suggested framework provides solid financial risk prediction.

The healthcare ROC curve is near to the diagonal reference line, indicating that the classifier has limited discriminative capacity for the designed healthcare-risk target. This behaviour is consistent with a ROC-AUC value of around 0.50, indicating the difficulty of forecasting the composite healthcare-risk label using existing patient data.

The urban ROC curve is above the random classifier and has a considerably larger area than the healthcare curve, indicating moderate discriminative skill. Although urban prediction remains more challenging than finance, the higher ROC-AUC over Sector FedAvg suggests that customized federated learning helps temporally changing environmental data by enhancing the ranking of future pollution-risk occurrences.

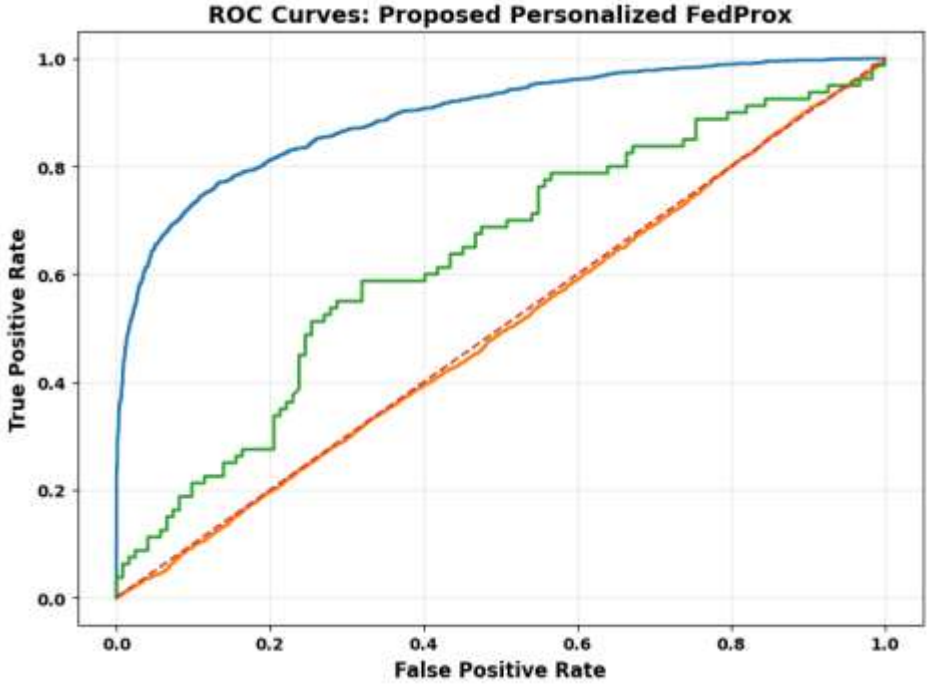

Figure 6. Receiver operating characteristic (ROC) curves of the proposed Personalized FedProx framework for the Finance, Healthcare, and Urban sectors.

4.9 Comparison of ROC-AUC Across Sectors

Figure 7 shows the mean ROC-AUC values with standard deviation error bars. The financial sector had the highest ROC-AUC for both techniques, at around 0.903 for the suggested methodology and 0.901 for Sector FedAvg. The healthcare ROC-AUC values were at 0.502 and 0.503, indicating that neither technique achieved meaningful discrimination. In the urban sector, the proposed technique had a much higher mean ROC-AUC of roughly 0.623 than Sector FedAvg, which was around 0.602.

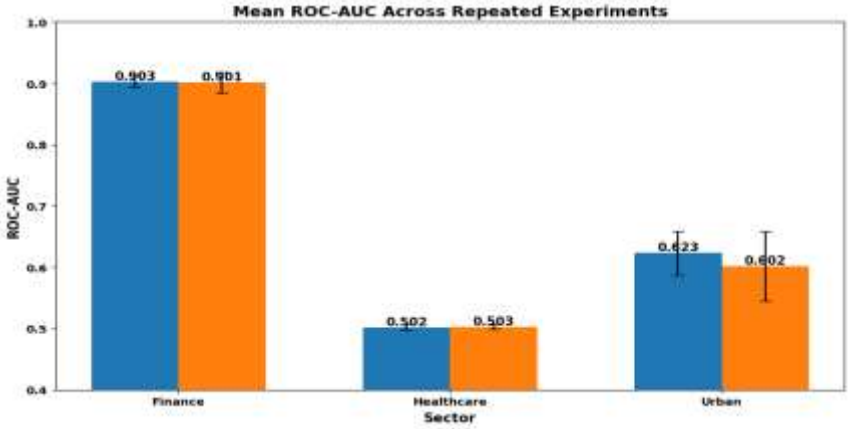

Figure 7. Mean ROC-AUC comparison between the proposed Personalized FedProx framework and Sector FedAvg across finance, healthcare, and urban-risk forecasting tasks. Error bars represent the standard deviation over five random seeds and three rolling urban folds.

Figure 7 indicates that predicted discrimination varies significantly between sectors. In the financial challenge, both techniques achieved high ROC-AUC values, showing that positive and negative loan-risk instances could be reliably separated. In contrast, the healthcare ROC-AUC stayed near 0.50, indicating that the available input features were insufficient to forecast the leakage-safe composite healthcare goal. The suggested strategy showed the greatest ROC-AUC improvement in the urban sector, where individualized adaptation and adaptive cross-sector aggregation raised the mean ROC-AUC from around 0.602 to 0.623.

4.10 Balanced-Accuracy Comparison

The balanced-accuracy figure gives a threshold-dependent comparison that equally considers both classes. Finance once again delivered the best results, with a balanced accuracy of 0.8193 for the proposed technique and 0.8229 for Sector FedAvg. Healthcare remained close to 0.50 across both methods. The proposed technique increased urban balanced accuracy slightly, from 0.5659 to 0.5707.

Figure 8 shows that the suggested framework did not consistently increase threshold-dependent classification performance. The finance baseline had somewhat greater balanced accuracy than the proposed method, however both healthcare models performed similarly to random classification. The urban sector showed minimal progress. These findings show that the suggested method's primary benefit is in maintaining cross-sector collaboration and boosting urban ranking performance, rather than attaining universal advances in class-level accuracy.

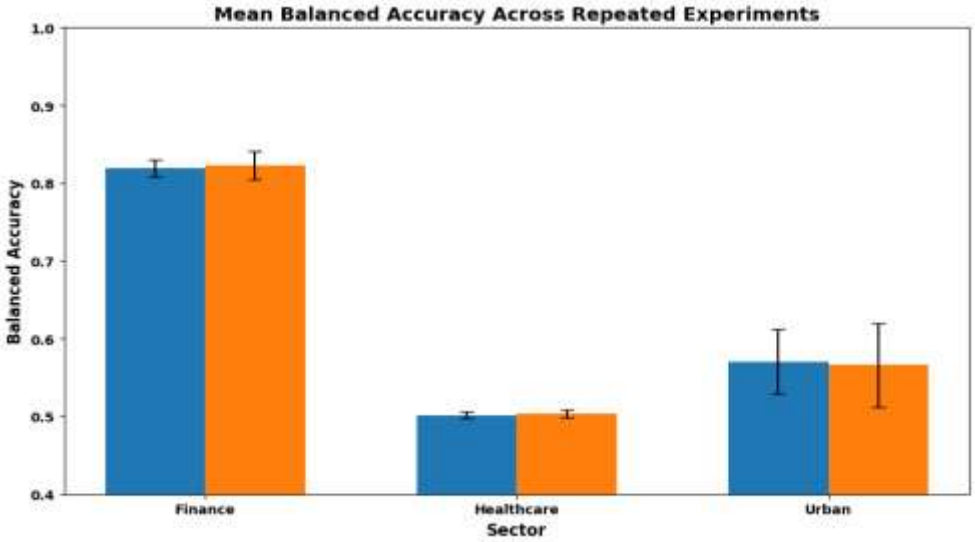

Figure 8. Mean balanced-accuracy comparison between the proposed Personalized FedProx framework and Sector FedAvg. Error bars show standard deviations across the repeated experiments.

4.11 Discussion of the Proposed Architecture

The experimental evidence somewhat backs up the motivation for the proposed architecture. The learnt sector-specific input adapters enable datasets with varying feature dimensions to enter a shared residual backbone, whilst the private residual adapters and prediction heads maintain sector specialization. Only the shared backbone is aggregated across sectors, with values of 0.30, 0.35, and 0.35 for banking, healthcare, and urban data, respectively. However, the data do not back up the assertion that the proposed technique regularly outperforms Sector FedAvg. Its advantages vary on the sector: Finance and healthcare performed similarly, with higher ordinary accuracy but no significant discriminative improvement. Urban areas showed modest but continuous mean gains, particularly in ROC-AUC and PR-AUC. The key contribution should thus be presented as a cross-sector personalized federated framework that limits negative transfer and provides selective benefits across disparate areas, rather than as a generally superior forecasting model. The gain analysis is especially essential. Out of the 18 sector-metric comparisons, the proposed approach resulted in positive mean increases in 12 cases, however several improvements were minor and happened in less than half of the runs. As a result, statistical significance testing would strengthen the analysis. A paired Wilcoxon signed-rank test or paired t-test could be used to compare the 15 matched runs for each sector and measure.

5. Limitations and Future Directions

One of the primary challenges is the heterogeneity of distributed datasets across finance, healthcare, and urban planning. Organizations typically collect, store, and manage data using different formats, feature representations, governance policies, and quality standards, resulting in non-independent and identically distributed (non-IID) data [30], [31]. Previous studies have emphasized that standardized data governance frameworks, explainable analytics, and scalable data integration mechanisms are essential for improving collaborative artificial intelligence systems and supporting reliable decision-making across heterogeneous environments [32] – [35]. Additionally, trust among participating organizations remains a major concern because institutions may be reluctant to collaborate without transparent governance and robust security guarantees [36] – [39]. Future research should therefore integrate federated learning with advanced privacy-preserving technologies such as differential privacy, secure multi-party computation, homomorphic encryption, blockchain-enabled auditing, and secure edge communication architectures to improve resilience while maintaining model utility and regulatory compliance [40] – [45].

Interpretability also remains a significant challenge for cross-sector risk forecasting. Decisions generated by AI models frequently influence financial investment strategies, healthcare interventions, insurance risk assessment, disaster preparedness, and urban infrastructure planning [46] – [49]. Although deep neural networks often outperform conventional machine learning algorithms, their black-box nature limits transparency and reduces stakeholder confidence. Decision-makers increasingly require interpretable predictions that clearly explain the factors influencing risk estimates [50] – [53]. Recent studies have demonstrated the value of explainable artificial intelligence in healthcare analytics, predictive medicine, precision agriculture, and intelligent decision-support systems for improving transparency, accountability, and user trust [54] – [57].

The proposed framework also focuses primarily on structured numerical information, whereas practical cross-sector risk forecasting increasingly depends on multimodal and continuously evolving data sources [51, 56]. Financial transactions, electronic health records, medical imaging, genomic profiles, wearable devices, IoT sensors, satellite imagery, environmental monitoring systems, transportation networks, and textual policy documents collectively provide complementary information for comprehensive risk assessment [58]–[63]. Recent advances in precision medicine, multi-omics integration, wearable health analytics, predictive intelligence, and environmental data analytics demonstrate that multimodal learning substantially improves prediction performance and supports more personalized decision-making [64] – [68].

Scalability also represents an important research challenge. As federated learning networks expand to include hundreds or thousands of participating organizations, communication overhead, synchronization latency, client heterogeneity, and resource constraints become increasingly significant. Smart city ecosystems continuously generate massive real-time data streams from edge devices, intelligent transportation systems, healthcare monitoring platforms, financial markets, and environmental sensors [69] – [71]. Developing communication-efficient optimization algorithms, adaptive client selection strategies, model framework, asynchronous aggregation techniques, and resource-aware edge intelligence will therefore be essential for enabling scalable, decision-making, and real-time cross-sector risk forecasting [72] – [75].

A previous study by Rahman et al. [76] also demonstrated the application of predictive analytics and machine learning to drug discovery and disease surveillance, highlighting the potential of data-driven

models for forecasting complex outcomes. In another study, Rahman et al. [77] integrated data analytics and machine learning into health informatics to examine clinical outcomes and pharmaceutical prescription patterns, providing a healthcare-focused basis for predictive risk modeling. Furthermore, Das et al. [78] explored IoT and big-data integration for real-time monitoring and decision-making in agro-food systems, demonstrating how distributed data sources can support resource management and predictive decision processes. In conclusion, these previous studies demonstrate a strong foundation in predictive analytics, machine learning, health informatics, and distributed data systems, providing a clear basis for extending this expertise toward federated machine learning for privacy-preserving, cross-sector risk forecasting in finance, healthcare, and urban planning.

6. Conclusion

This study described a personalized federated learning system for collaborative risk forecasting in diverse financial, healthcare, and urban planning sectors. Unlike traditional federated learning approaches, which rely on fully shared models, the proposed framework combines sector-specific input adapters, a shared residual backbone, private residual adapters, and task-specific prediction heads to balance collaborative knowledge transfer with domain-specific specialization. Furthermore, adaptive sector-weighted aggregation and FedProx regularization were used to increase optimization stability in the presence of heterogeneous data distributions while conserving sector-specific information.

The framework was tested on publically available datasets using a repeated experimental approach with five random seeds and three rolling temporal folds for the urban dataset. Experimental results showed that the suggested technique performed similarly to the Sector FedAvg baseline in financial risk forecasting while offering consistent improvements in urban forecasting, particularly in ROC-AUC and PR-AUC. In healthcare, the suggested framework improved overall classification accuracy, but the prediction job remained difficult due to the leakage-safe composite objective and the limited discriminative information provided in the input features. Overall, the findings show that personalized federated learning can effectively promote collaborative learning across diverse domains while lowering the risk of negative transfer that comes with completely shared federated models.

Although the suggested approach yields promising findings, numerous drawbacks remain. The evaluation only looked at three application fields and binary risk prediction tasks, although healthcare performance suggests that further clinical features or other target formulations may be needed for better discrimination. Future research will look into dynamic aggregation strategies, attention- or transformer-based shared backbones, explainable federated learning, statistical significance analysis across repeated experiments, and the application of the proposed framework to new domains and multiclass risk prediction problems.

Funding
This research received no external funding.

Conflicts of Interest
The authors declare no conflict of interest.

ORCID
Md Arif Hossain: https://orcid.org/0009-0003-1815-0920
S M Arif Al Sany: https://orcid.org/0009-0005-2792-6510
Ridwanur Rahman: https://orcid.org/0009-0006-8951-0956
Molla Al Rakib Hasan: https://orcid.org/0009-0009-9676-1026

References

[1] Ayeelyan, J., Utomo, S., Rouniyar, A., Hsu, H. C., & Hsiung, P. A. (2024). Federated learning design and functional models: Survey. Artificial Intelligence Review, 58(1), 21.
[2] Zhang, Y., Zeng, D., Luo, J., Fu, X., Chen, G., Xu, Z. and King, I., 2024. A survey of trustworthy federated learning: Issues, solutions, and challenges. ACM Transactions on Intelligent Systems and Technology, 15(6), pp.1-47.
[3] Guo, W., Zhuang, F., Zhang, X., Tong, Y., & Dong, J. (2024). A comprehensive survey of federated transfer learning: challenges, methods and applications. Frontiers of Computer Science, 18(6), 186356.
[4] Wu, J., Dong, F., Leung, H., Zhu, Z., Zhou, J., & Drew, S. (2024). Topology-aware federated learning in edge computing: A comprehensive survey. ACM Computing Surveys, 56(10), 1-41.
[5] Fan, B., Jiang, S., Su, X., Tarkoma, S., & Hui, P. (2024, December). A survey on model-heterogeneous federated learning: Problems, methods, and prospects. In 2024 IEEE international conference on big data (BigData) (pp. 7725-7734). IEEE.

[6] Yang, H., Li, J., Hao, M., Zhang, W., He, H. and Sangaiah, A.K., 2024. An efficient personalized federated learning approach in heterogeneous environments: a reinforcement learning perspective. Scientific Reports, 14(1), p.28877.
[7] Tang, X., Guo, S., Zhang, J. and Guo, J., 2024, May. Learning personalized causally invariant representations for heterogeneous federated clients. In International Conference on Learning Representations (Vol. 2024, pp. 10016-10037).
[8] Xie, L., Lin, M., Xu, C., Luan, T., Zeng, Z., Qian, W., ... & Wu, Z. (2024, October). Mh-pflgb: Model heterogeneous personalized federated learning via global bypass for medical image analysis. In International Conference on Medical Image Computing and Computer-Assisted Intervention (pp. 534-545). Cham: Springer Nature Switzerland.
[9] Liu, B., Lv, N., Guo, Y., & Li, Y. (2024). Recent advances on federated learning: A systematic survey. Neurocomputing, 597, 128019.
[10] ZHANG, C., & LI, W. (2025). Survey of federated learning in healthcare: Applications, challenges, and future directions. Chinese Journal of Engineering, 47(9), 1825-1840.
[11] Ye, M., Fang, X., Du, B., Yuen, P. C., & Tao, D. (2023). Heterogeneous federated learning: State-of-the-art and research challenges. ACM Computing Surveys, 56(3), 1-44.
[12] Gao, D., Yao, X., & Yang, Q. (2022). A survey on heterogeneous federated learning. arXiv preprint arXiv:2210.04505.
[13] Tan, A. Z., Yu, H., Cui, L., & Yang, Q. (2022). Towards personalized federated learning. IEEE transactions on neural networks and learning systems, 34(12), 9587-9603.
[14] Weimann, E. (2025). Federated Learning with Model Personalization: A Survey.
[15] Pais, V., Rao, S., & Muniyal, B. (2025). Healthcare federated learning: a survey of applications and frameworks. International Journal of Computers and Applications, 47(6), 532-551.
[16] Madathil, N.T., Dankar, F.K., Gergely, M., Belkacem, A.N. and Alrabaee, S., 2025. Revolutionizing healthcare data analytics with federated learning: A comprehensive survey of applications, systems, and future directions. Computational and Structural Biotechnology Journal, 28, pp.217-238.
[17] Nasajpour, M., Pouriyeh, S., Parizi, R. M., Han, M., Mosaiyebzadeh, F., Liu, L., ... & Batista, D. M. (2025). Federated learning in smart healthcare: A survey of applications, challenges, and future directions. Electronics, 14(9), 1750.
[18] Thakur, A., Molaei, S., Nganjimi, P. C., Liu, F., Soltan, A., Schwab, P., ... & Clifton, D. A. (2024). Knowledge abstraction and filtering based federated learning over heterogeneous data views in healthcare. npj Digital Medicine, 7(1), 283.
[19] Cheng, H., Qu, Y., Liu, W., Gao, L., & Zhu, T. (2025). Decentralized federated learning for private smart healthcare: A survey. Mathematics, 13(8), 1296.
[20] Howlader, S. R. K., Liu, L., Chen, X., Wu, H., Yuan, B., & Bhattacharjee, A. (2026). Federated learning applications in healthcare informatics: A comprehensive review. ACM Computing Surveys, 58(12), 1-48.
[21] Gayen, A., Das, R., Mondal, A., Singha, S., & Jana, A. (2026). A survey: Federated learning in healthcare. Computers and Electrical Engineering, 135, 111195.
[22] Wang, F., Tang, H., & Li, Y. (2023). Factor-assisted federated learning for personalized optimization with heterogeneous data. arXiv preprint arXiv:2312.04281.
[23] Molaei, S., Thakur, A., Clifton, L., Soltan, A., Schwab, P., Belgrave, D., ... & Clifton, D. A. (2025). Learning Across the Divide: Personalised Federated Learning for Robust Clinical Modelling under Data-View Heterogeneity. IEEE Journal of Biomedical and Health Informatics.
[24] Kim, J., Kim, J., Hur, K., & Choi, E. (2026). Federated learning for heterogeneous electronic health record systems with cost effective participant selection. Scientific Reports.
[25] Noor, A., Chaman, U. M., & Kabir, M. S. (2026). Federated learning in healthcare: A comprehensive survey on privacy, scalability and clinical applications. ICT Express.
[26] Kirupa Shankar, K. M., & Santhi, V. (2026). Privacy-adaptive end-to-end federated learning framework with self-learning differential privacy and personalized optimization for secure healthcare intelligence. Complex & Intelligent Systems, 12(4), 1.
[27] Zhu, H., Togo, R., Ogawa, T., & Haseyama, M. (2026). Personalized federated learning for medical vision-language models via efficient fine-tuning and uncertainty-aware disentanglement. Journal of Biomedical Informatics, 105014.
[28] Xie, Z., & Zhang, L. (2026). FedAttn-Credit: attention-augmented federated learning with adaptive differential privacy for rural inclusive finance credit assessment. Scientific Reports.
[29] Huda, S. A., Canzaniello, M., Annunziata, D., & Piccialli, F. (2026). Graph-based federated learning for smart healthcare: A comprehensive survey. Future Generation Computer Systems, 108524.

[30] Ahmed, M. K., Rozario, E., Mohonta, S. C., Ferdousmou, J., Saimon, A. S. M., Moniruzzaman, M., Manik, M. M. T. G., & Hasan, R. (2025). Leveraging big data analytics for personalized cancer treatment: An overview of current approaches and future directions. Journal of Engineering. https://doi.org/10.1155/je/9928467

[31] Alam, K. R., Saurav, K. R. H., Kabir, J. U. Z., Rahman, M. S., Hasan, M. I., & Barua, C. (2024). AI-driven digital marketing analytics and leadership strategies for sustainable business innovation: A mixed-methods research study. The American Journal of Management and Economics Innovations, 6(12), 83–102. Retrieved from https://theamericanjournals.com/index.php/tajmei/article/view/7400

[32] Alam, M. I., Hemal, M. A. K. P., Sami, M. A., & Rahman, M. L. (2024). Robust and Interpretable Crop Recommendation: A Case Study on a Balanced Multi-crop Agronomic Dataset. European Journal of Ecology, Biology and Agriculture, 1(5), 168-184. https://doi.org/10.59324/ejeba.2024.1(5).14

[33] Sami, M. A., Rahman, M. L., Tanni, Z. A., Munmun, Z. S., Nusrat, S., & Biswas, B. (2026). Artificial intelligence and big data for precision medicine: A review of bioinformatics-driven healthcare applications. Frontiers in Computer Science and Artificial Intelligence, 5(6), 36–43. https://doi.org/10.32996/fcsai.2026.5.6.7

[34] Saurav, K. R. H., Alam, K. R., Barua, C., Hasan, M. I., Rahman, M. S., & Kabir, J. U. Z. (2023). AI-Driven Consumer Behavior Insights and Human-Centered Marketing Strategies for Enhancing Engagement and Innovation. Journal of Business and Management Studies, 5(6), 187-197. https://doi.org/10.32996/jbms.2023.5.6.16x

[35] Shone, N., Ngoc, T. N., Phai, V. D., & Shi, Q. (2018). Deep learning approach for intrusion detection system. IEEE Transactions on Emerging Topics in Computational Intelligence, 2(1), 41–50.

[36] Sicari, S., Rizzardi, A., Grieco, L. A., & Coen-Porisini, A. (2015). Security, privacy and trust in IoT. Computer Networks, 76, 146–164.

[37] Alam, M. I., Sami, M. A., Al Masud, A., Ahmed, H., & Hossain, F. (2025). AI-Driven Big Data Analytics for Personalized Cancer Treatment: Integrating Multi-Omics, Medical Imaging, and Predictive Intelligence. Journal of Computer Science and Technology Studies, 7(11), 428-441. https://doi.org/10.32996/jcsts.2025.7.11.40

[38] Alam, M. I., Sami, M. A., Hemal, M. A. K. P., & Rahman, M. L. (2023). Predictive Analytics and Decision Intelligence for Climate-Resilient Agritech Systems. Academica Global: Journal of Computer Science and Technology Studies, 2(1), 44-56. https://doi.org/10.32996/agjcsts.2023.2.1.4

[39] Alam, M. I., Sikder, T. R., Sami, M. A., Rahman, M. L., Hemal, M. A. K. P., Linkon, A. A., Bhuiyan, M. M. R., Aziz, M. M., Islam, M. S., & Rahman, M. M. (2026). A robust and explainable approach to crop recommendation using a balanced multi-crop agronomic dataset. Journal of Environmental and Agricultural Studies, 7(3), 1-15. https://doi.org/10.32996/jeas.2026.7.3.1

[40] Ashik, A. A. M., Rahman, M. M., Hossain, E., Rahman, M. S., Islam, S., & Khan, S. I. (2023). Transforming U.S. Healthcare Profitability through Data-Driven Decision Making: Applications, Challenges, and Future Directions. European Journal of Medical and Health Research, 1(3), 116-125. https://doi.org/10.59324/ejmhr.2023.1(3).21

[41] Yin, C., Zhu, Y., Fei, J., & He, X. (2017). A deep learning approach for intrusion detection using recurrent neural networks. IEEE Access, 5, 21954–21961.

[42] Yusuf, M. A., Chowdhury, N. M., Rone, P. D., Saha, P. P., Hossan, M. I., Sarkar, D., Paul, R., Hossain, M. R., & Chakraborty, M. (2025). Advancing Public Safety with Real-Time Life Jacket Detection and Demographic Profiling Using YOLOv8 and Age Classification. EAI Endorsed Trans AI Robotics. 4.1-12. https://doi.org/10.4108/airo.9785. Available from: https://publications.eai.eu/index.php/airo/article/view/978z5

[43] Saha, P. P., Paul, R., Khan, M. R. K., Siddique, N. A. S., & Sarker, B. D. (2026). AI-driven modernization of Medicare and Medicaid enterprise systems: Interoperability, claims analytics, and fraud detection frameworks. Journal of Intelligent Decision Making and Information Science, 3(5s), 827–866. https://doi.org/10.59543/jidmis.v3.1223

[44] Barua, C., M. S., Rahman, M. S., Hasan, M. I., Saurav, K. R. H., Alam, K. R., & Kabir, J. U. Z. (2024). AI-driven digital twin frameworks for predictive maintenance and process optimization in smart battery manufacturing for electric vehicles. Academica Global: Journal of Computer Science and Technology Studies, 3(1), 39–51. https://doi.org/10.32996/agjcsts.2024.3.1.4

[45] Barua, C., Rahman M. S., Hasan M. I., Saurav K. R. H., Alam K. R., & Kabir J. U. Z. (2024). AI-Driven Digital Twin Frameworks for Predictive Maintenance and Process Optimization in Smart Battery Manufacturing for Electric Vehicles. Academica Global: Journal of Computer Science and Technology Studies, 3(1), 39-51. https://doi.org/10.32996/agjcsts.2024.3.1.4

[46] Saha, P. P., Rone, P. D., Sarkar, D., Yusuf, M. A., Hossan, M. I., & Mazumder, M. S. J. (2025). Advancing carbon emission prediction through machine learning: The impact of fossil, nuclear, and renewable

energies. In 2025 International Conference on Emerging Smart Computing and Informatics (ESCI) (pp. 1–7). IEEE. https://doi.org/10.1109/ESCI63694.2025.10988213

[47] Mondal, R. S., Purba, T. N., Purba, N. N., Rahman, M. M., & Sikder, T. R. (2026b). AI-Driven Glycemic Instability Risk Modeling for Proactive Intervention and Chronic Disease Management in U.S. Healthcare Systems. Journal of Medical and Health Studies, 7(1), 29-43. https://doi.org/10.32996/jmhs.2023.4.6.21

[48] Sikder, T. R., Dash, S., Uddin, B., & Hossain, F. (2023a). AI-Powered Data Analytics and Multi-Omics Integration for Next-Generation Precision Oncology and Anticancer Drug Development. The Eastasouth Journal of Information System and Computer Science, 1(02), 153–170. https://doi.org/10.58812/esiscs.v1i02.838

[49] Sikder, T. R., Sayeed, N., Hossain, M. J., Faruk, M. I., Alam, M. I., Uddin, S. M. M., & Adnan, M. (2025). AI-Driven Environmental Precision Oncology: Integrating Big Data, Multi-Omics, Medical Imaging, and Exposomic Intelligence for Personalized Cancer Care. International Journal of Computational and Experimental Science and Engineering, 11(4). https://doi.org/10.22399/ijcesen.4533

[50] Sikder, T. R., Siam, M. A., Melon, M. M. H., Uddin, S. M. M., Mohonta, S. C., & Karim, F. (2023b). A Multimodal Data Analytics Framework for Early Cancer Detection Using Genomic, Radiomic, and Clinical Big Data Fusion. Journal of Computer Science and Technology Studies, 5(3), 183-188. https://doi.org/10.32996/jcsts.2023.5.3.13

[51] Sommer, R., & Paxson, V. (2010). Outside the closed world: On using machine learning for network intrusion detection. IEEE Symposium on Security and Privacy, 305–316.

[52] Nusrat, S., Hossain, F., & Sikder, T. R. (2024). Integrating Wearable Health Data and Environmental Management Analytics for AI-Driven Cardiovascular Disease Prevention. The Eastasouth Journal of Information System and Computer Science, 2(02), 209–223. https://doi.org/10.58812/esiscs.v2i02.868

[53] Rahman, M. L., Alam, M. I., Anzum, R., Acharjee, S., Alam, M. S., & Shamarukh, S. (2026). AI-driven predictive analytics for supply chain resilience, financial risk management, and digital marketing strategy: A unified business intelligence framework. Journal of Business and Management Studies, 8(7), 41–55. https://doi.org/10.32996/jbms.2026.8.7.3

[54] Saha, P. P., Rahaman, M. M., Islam, M. T., & Chowdhury, N. I. (2025). Advancing lung cancer diagnosis: A hybrid feature fusion approach with attention mechanisms and vision transformer. In 2025 2nd International Conference on Intelligent Systems for Cybersecurity (ISCS) (pp. 1–7). IEEE. https://doi.org/10.1109/ISCS69371.2025.11386016

[55] Gangula, U. K. R., Miah, M. A., Mula, K., Dhakan, M., Sadat, Q. T., & Nayak, S. (2026). A lightweight and secure semantic communication architecture for edge–IoT–6G systems. IEEE Communications Standards Magazine.

[56] Hossain, E., Shital, K. P., Rahman, M. S., Islam, S., Khan, S. I., & Ashik, A. A. M. (2024). Machine learning-driven governance: Predicting the effectiveness of international trade policies through policy and governance analytics. Journal of Trends in Financial and Economics, 1(3), 50–62. https://doi.org/10.61784/jtfe3053

[57] Islam, S., Hossain, E., Rahman, M. S., Rahman, M. M., Khan, S. I., & Ashik, A. A. M. (2023). Digital Transformation in SMEs: Unlocking Competitive Advantage through Business Intelligence and Data Analytics Adoption. 5 (6):177-186. https://doi.org/10.32996/jbms.2023.5.6.14

[58] Kabir, J. U. Z., Saurav, K. R. H., Rahman, M. S., Hasan, M. I., Barua, C., Alam, K. R., & Rahman, M. M. (2023). Financially sustainable strategic leadership and management with predictive analytics to strengthen nationwide U.S. healthcare quality and performance. European Journal of Medical and Health Research, 1(3), 144–150. Eur J Med Health Res, 2023;1(3):144-50. DOI: 10.59324/ejmhr.2023.1(3).24

[59] Yusuf, M. A., Khan, M. R. K., Saha, P. P., & Rahaman, M. M. (2024). Data fusion of semantic and depth information in the context of object detection. In 2024 Second International Conference on Intelligent Cyber Physical Systems and Internet of Things (ICoICI) (pp. 1124–1129). IEEE. https://doi.org/10.1109/ICoICI62503.2024.10696627

[60] Kaur, J., Prabha, M., Samiun, M., Hasan, S. N., Hasan, R., Esa, H., et al. (2025). Comparative analysis of transformer and LSTM architectures for cybersecurity threat detection using machine learning. EAI Endorsed Transactions on AI and Robotics, 4. https://publications.eai.eu/index.php/airo/article/view/9759

[61] Khair, F. B., Saimon, A. S. M., Hossain, S., et al. (2025). Deep neural network-based imaging system for efficient pancreatic tumor identification. Intelligent Decision Technologies, 19(6), 4118–4129. https://doi.org/10.1177/18724981251381581

[62] Mahin, M. R. H., Chakraborty, P., Das, N., Kaur, H., Himel, H. U., Kaur, J., & Mohapatra, A. G. (2026). Secured and standardized intelligent zero-touch 6G framework for edge-AI applications. IEEE Communications Standards Magazine. https://doi.org/10.1109/MCOMSTD.2026.3660159

[63] Manik, M. M. T. G., Saimon, A. S. M., Ahmed, M. K., Hossain, S., Moniruzzaman, M., & Islam, M. S. (2025). Predictive modelling for early detection of type 2 diabetes using AI-driven machine learning algorithms and big data analytics. In J. C. Bansal, P. Jamwal, & S. Hussain (Eds.), Lecture Notes in Networks and Systems (Vol. 1629). Springer. https://doi.org/10.1007/978-3-032-05548-4_33

[64] Mondal, R. S., Ahmed, R. A., Hemal, M. A. K. P., Sikder, T. R., & Juie, B. J. A. (2026a). A Multi-Omics Transformer Foundation Model For AI-Driven Early Cancer Detection Using cfDNA And cfRNA: Implications For Precision Oncology And Early Intervention In U.S. Healthcare Systems. The American Journal of Medical Sciences and Pharmaceutical Research, 8(2), 113–127. https://doi.org/10.37547/tajmspr/Volume08Issssue02-17

[65] Hasan, M. I., Barua, C., Rahman, M. S., Alam, K. R., Kabir, J. U. Z., & Saurav, K. R. H. (2023). Resilient healthcare and critical urban infrastructure design using AI-driven engineering and project management systems. Journal of Medical and Health Studies, 4(6), 20–34. https://doi.org/10.32996/jmhs.2023.4.6.20

[66] Hasan, M. M., Alam, M. I., Chowdhury, M. A. H., & Anwar, M. M. (2026). AI-Driven Big Data Analytics for Precision Medicine and Healthcare Intelligence: A Unified Framework for Cancer, Chronic Disease, and Clinical Decision Optimization. Frontiers in Computer Science and Artificial Intelligence, 5(2), 41-62. https://doi.org/10.32996/jcsts.2026.5.1.5

[67] Sami, M. A., Hemal, M. A. K. P., Alam, M. I., & Rahman, M. L. (2024). Data Governance and Analytics Infrastructure for Scalable Decision-Making in Development and Agritech Programs. European Journal of Applied Science, Engineering and Technology, 2(2), 388-403. https://doi.org/10.59324/ejaset.2024.2(2).28

[68] Habib, M. R., Yusuf, M. A., Warnasuriya, W. M. H. N., Sunny, K., Rahaman, M. M., & Khan, M. R. K. (2024). A comprehensive review on the advancement of home automation system. In 2024 Second International Conference on Intelligent Cyber Physical Systems and Internet of Things (ICoICI) (pp. 638–642). IEEE. https://doi.org/10.1109/ICoICI62503.2024.10696135

[69] Vanu, N., Hasan, M. R., Sikder, T. R., & Tamanna, Z. S. (2021). AI-Driven Big Data Analytics for Precision Medicine: A Unified Framework Integrating Molecular Data Intelligence, Wearable Health Systems, and Predictive Modeling. Journal of Computer Science and Technology Studies, 3(2), 124-141. https://doi.org/10.32996/jcsts.2021.3.2.11

[70] Varanasi, S. R., Valiveti, S. S. S., Adnan, M., Faruk, M. I., Hossain, M. J., & Manik, M. M. T. G. (2026). Cross-domain standardization and secure edge intelligence for real-time digital twin deployments in next-generation communication systems. IEEE Communications Standards Magazine. https://doi.org/10.1109/MCOMSTD.2026.3662187.

[71] Hemal, M. A. K. P., Sayeed, N., Sami, M. A., Alam, M. I., Sikder, T. R., Dipa, S. A., & Rahman, M. L. (2025). Leveraging Data Analytics to Strengthen Public Health and Global Economic Sustainability. European Journal of Medical and Health Research, 3(4), 253- 263. https://doi.org/10.59324/ejmhr.2025.3(4).37

[72] Hossain, E., Ashik, A. A. M., Rahman, M. M., Khan, S. I., Rahman, M. S., & Islam, S. (2023). Big data and migration forecasting: Predictive insights into displacement patterns triggered by climate change and armed conflict. Journal of Computer Science and Technology Studies, 5(4): 265–274. https://doi.org/10.32996/jcsts.2023.5.4.27.

[73] Ayrin, F. J., Rahman, M. M., Quader, M. A., Dass, A., Khondaker, M. M. H., Chakraborty, M., Saha, P. P., Khan, M. R. K., Akuthota, V., & Anwar, A. S. (2025). MentalLLM: A transformer-based large language model framework for depression detection. 2025 IEEE International Women in Engineering (WIE) Conference on Electrical and Computer Engineering (WIECON-ECE), 61–65. https://doi.org/10.1109/WIECON-ECE69386.2025.11525902.

[74] Islam, A., Rana, M. S., Karim, F., Biplob, M. Y., Sami, M. A., Rahman, M. L., & Shamarukh, S. (2026). Real-time, multi-modal artificial intelligence for Medicare fraud detection: An integrated framework combining claims, electronic health records, and provider behavioral signals. International Journal of Advances in Signal and Image Sciences, 12(5). https://doi.org/10.29284/z691dz32.

[75] Hossain, M. J., Bakhsh, M. M., Sami, M. A., Alam, M. I., Melon, M. M. H., & Manik, M. M. T. G. (2026). Self-adaptive artificial intelligence systems for large-scale data-driven decision making. 2026 IEEE International Conference for Convergence in Computing Technology (I3CTCON). https://doi.org/10.1109/I3CTCON68242.2026.11507252.

[76] Das, K., Tanvir, A., Rani, S., & Aminuzzaman, F. M. (2025). Revolutionizing agro-food waste management: Real-time solutions through IoT and big data integration. Voice of the Publisher, 11(1), 17–36. https://doi.org/10.4236/vp.2025.111003.

[77] Rahman, M. M., Juie, B. J. A., Tisha, N. T., & Tanvir, A. (2022). Harnessing predictive analytics and machine learning in drug discovery, disease surveillance, and fungal research. Eurasia Journal of Science and Technology, 4(2), 28–35. https://doi.org/10.61784/ejst3099.

[78] Rahman, M. M., Rahman, M. S., Islam, S., Khan, S. I., Ashik, A. A. M., Hossain, E., & Tanvir, A. (2025). Integrating data analytics into health informatics: Advancing equity, pharmaceutical outcomes, and public health decision-making. Eurasian Journal of Medicine and Oncology, 9(4), 284–295. https://doi.org/10.36922/EJMO025300319.